

# Straightforward energetic approach to studies of the corrosion behaviour of nano-copper thin-layer coatings

Maria Trzaska · Zdzislaw Trzaska

Received: 13 February 2007 / Revised: 22 May 2007 / Accepted: 25 May 2007 / Published online: 27 June 2007  
© Springer Science+Business Media B.V. 2007

**Abstract** This paper presents a one-period energy method of studying the electrochemical corrosion phenomena that occur on metal surfaces. The method employs the energy state variables (time functions) to determine whether the material is susceptible to corrosion. The main feature of this approach is the elimination of the frequency analysis, and thereby gives significant simplifications of the corrosion rate measurement. Another important feature is that the method is based on an analysis of the appropriate loops on the energy phase plane which results in the corrosion process being easily estimated through the evaluation of the loop area. The physical results obtained by this method are easily interpretable with robust properties. The usefulness of the proposed technique was examined in microcrystalline and nanocrystalline copper layers deposited on a polycrystalline substrate by the electrocrystallization method. The quantitative results obtained from the measurements of the one-period energy loops are used for controlling the corrosion resistances of the micro- and nano-copper thin-layer coatings. Several experiments performed on real specimens verified the effectiveness of the method as used for analysing the electrochemical corrosion in many practical systems. We have shown that the corrosion resistance of the nanocrystalline copper layers is worse than that of microcrystalline copper layers even

when the layers of the two types are produced by the same electrochemical method.

**Keywords** Corrosion · Electrocrystallization · Nanocrystalline and microcrystalline copper layers · One-period energy loops

## 1 Introduction

Recently, several methods have been proposed for evaluating the susceptibility of various metal coatings to electrochemical corrosion. The development of various techniques for studying the mechanisms of corrosion and corrosion protection has, on the one hand, brought quite satisfactory results, but, on the other hand, they have aroused a lot of critical remarks as to the interpretation of the differences between individual physical models [1–6]. Even simple models appeared to be controversial [7, 8]. Among the various electrochemical methods suitable for measuring the corrosion rate of metals, the harmonic current analysis method is useful since the corrosion current can be calculated without the use of Tafel constants at the corrosion potential. Significant advances in the study on the mechanisms of corrosion and corrosion protection have been achieved since the development of impedance measurements. The measurements have been expanded to the study of mass transport and stress corrosion cracking, as well as to a noise analysis used for studying localized corrosion, stress corrosion cracking and blistering of coatings [9–15]. In particular, the impedance measurements permit separating the consecutive elementary steps involved in the overall process, and increasing the knowledge of the mechanisms and progress of corrosion, as well as improving the measures of anti-corrosion protec-

---

M. Trzaska (✉)  
Department of Materials Science and Engineering, Warsaw  
University of Technology, Plac Politechniki 1, Warsaw 00-661,  
Poland  
e-mail: matr@inmat.pw.edu.pl

Z. Trzaska  
Department of Electrical Engineering, Warsaw University of  
Technology, Plac Politechniki 1, Warsaw 00-661, Poland  
e-mail: zdzislaw.trzaska@netlandia.pl

tion [16–23]. During recent years, many online monitoring methods have been used and several newer techniques have been investigated. This research line has great significance since there is no technique that can be employed alone in all practical situations.

Although the methods utilizing linear polarization resistance and electrical impedance are commonly used for online monitoring they have certain limitations. They either require prior knowledge of Tafel constants or can only be used where uniform corrosion takes place. The measurement of the interfacial impedance values at low and high frequencies has been suggested as an alternative. The results obtained by this method are however complicated and their interpretation becomes difficult if more than one time constant is involved.

In this paper we utilize the results reported in refs. [9–11, 14, 15] in the corrosion measurements and analyze them in the context of the activation energy and mass transfer effects. The ability to transfer the anodic and cathodic charges determines the nature and magnitude of the corrosion reaction.

## 2 One-period energy approach

In many electrochemical systems, the data collection procedure may interfere with the electrochemical process. To avoid this it is recommended to use small AC signals and not to introduce a DC potential difference across the system, since it can induce a further electrochemical activity. Using small periodic excitations and assuming that the system time response is also periodic, we can evaluate the energy absorbed during the corrosion process [2–4, 17, 24].

The steady state energy  $W(\Delta t)$  delivered by the source  $v(t)$  to the corrosion system during the time interval  $\Delta t = nT$ , ( $T$  is the period,  $n \gg 0$  is a positive integer) is expressed by

$$W(\Delta t) = nW_T \quad (1)$$

where  $W_T$  denotes the one-period energy delivered by the source. Thus, in the periodic state, it is sufficient to evaluate  $W_T$ , and multiply it by  $n$  to obtain the energy absorbed by the corrosion element during the given time interval  $\Delta t$ . A schematic representation of this situation is shown in Fig. 1. Deriving the corresponding expression for  $W_T$ , we obtain

$$\begin{aligned} W_T &= \int_0^T v(t)i(t)dt = \int_0^T v(t) \frac{d}{dt} \left( \int i(\tau)d\tau \right) dt \\ &= \int_{q(0)}^{q(T)} v(t)dq(t) = \int_{\psi(0)}^{\psi(T)} i(t)d\psi(t) \end{aligned} \quad (2)$$

where

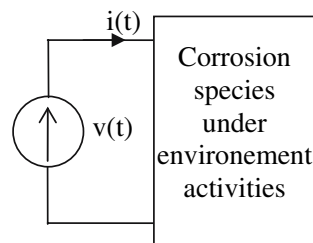


**Fig. 1** Corrosion species in the periodic energy state

$$q(t) = \int i(t)dt \quad \text{and} \quad \psi(t) = \int v(t)dt \quad (3)$$

are the electric charge and magnetic flux delivered by the source  $v(t)$ , respectively.

It follows from (2) and (3) that the area enclosed by a one-period loop in the energy phase plane with coordinates  $(v(t), q(t))$  or, equivalently,  $(\psi(t), i(t))$ , determines the one-period energy  $W_T$  delivered to the controlled element that operates under periodic non-harmonic conditions [25–30].

It is worth noting that it does not matter which energy phase plane we choose to determine  $W_T$ . In some cases it is easier to evaluate the phase variable  $q(t)$  whereas in other—the phase variable  $\psi(t)$  is more suitable. Thus, for any arbitrary corrosion specimen operating under periodic non-sinusoidal conditions it is possible to determine directly the one-period energy  $W_T$  without the necessity of using the power- or the Fourier series approach [24, 29, 31–33].

Another important feature of the one period energy approach is the easy way of evaluating the surface area enclosed by the loop in the energy phase plane. In most applications we have preliminary knowledge of the forms of the physical system response to a given input. This allows us to choose a priori the energy phase plane most appropriate for the calculations. Moreover, the calculation results can be easily interpreted and have robust properties.

To illustrate the main feature of the one-period energy approach let us consider the case of harmonic problems using a linear corrosion model with a sinusoidal waveform source. Fig. 2 illustrates the case with  $v(t) = V\sqrt{2} \cos(\omega t)$ , where  $V$  is the *rms* value of  $v(t)$ . Let the current  $i(t)$  be the system output of the form

$$i(t) = I\sqrt{2} \cos(\omega t - \varphi) \quad (4)$$

where  $\varphi$  is the phase shift.

If  $i(t)$  is taken to be one coordinate of the energy phase plane, then the magnetic flux

$$\psi(t) = \int v(t)dt = -\frac{V\sqrt{2}}{\omega} \sin(\omega t) \quad (5)$$

should be chosen to be the second coordinate.

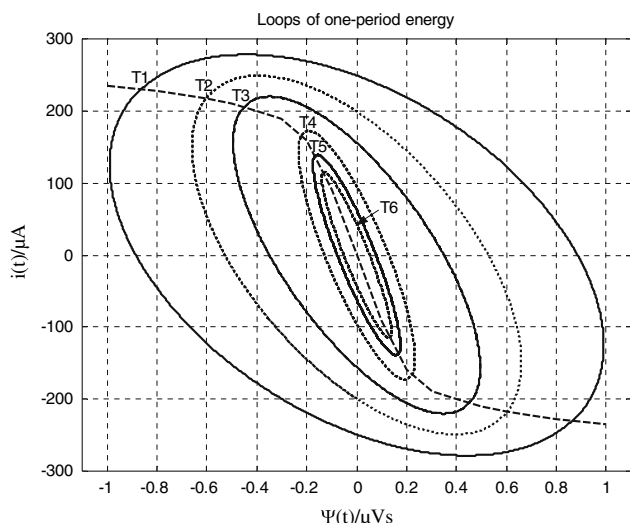


**Fig. 2** Illustration of one-period energy loops

Thus the one-period energy of the network is given by

$$W_T = \int_{\psi(0)}^{\psi(T)} i(t) d\psi(t) \tag{6}$$

To derive an explicit expression for the one-period energy loop we find an appropriate relationship between  $i(t)$  and  $\psi(t)$  and eliminate the time variable. Thus we have

$$\sin(\omega t) = \frac{-\omega\psi(t)}{V\sqrt{2}}, \quad \text{and} \quad \cos(\omega t) = \sqrt{1 - \left(\frac{-\omega\psi(t)}{V\sqrt{2}}\right)^2} \tag{7}$$

Next, substituting (7) in (4) and simplifying the respective terms we obtain the ellipse

$$\left(\frac{i(t)}{a}\right)^2 + \left(\frac{\psi(t)}{b}\right)^2 = 1 \tag{8}$$

where

$$a = \frac{I\sqrt{2} \cos \varphi}{\sqrt{1 + \sin \varphi}} \quad \text{and} \quad b = \frac{V\sqrt{2} \cos \varphi}{\omega\sqrt{1 - \sin \varphi}} \tag{9}$$

define the semi-axes in the one-period energy phase plane.

Now, we would like to find the surface area  $S$  enclosed by the ellipse (8). It is well known that  $S = \pi ab$  and, thus, substituting (9) here, we obtain

$$S = \frac{2\pi}{\omega} \frac{VI \cos^2 \varphi}{\sqrt{1 - \sin^2 \varphi}} = T VI \cos \varphi \tag{10}$$

Since  $P = VI \cos \varphi$  is the active power that operates in the system, and  $T = 2\pi / \omega$  defines the period, we easily find from (10) that  $S = W_T$ .

Thus the surface area of the ellipse in the energy phase plane ( $i(t), \psi(t)$ ) defines the one-period energy delivered by the harmonic source to its load which operates under linear conditions of the corrosion processes. By way of example, the variations of the one-period energy during the successive stages of the corrosion process induced by a small-amplitude sine input are shown in Fig. 3. The process was monitored by measuring the currents  $i(t)$  every 5 min during a 30 min period.

The proposed approach can easily be applied to any periodic waveforms including discontinuous.

The patterns shown in Fig. 3 correspond to the processes  $p_1 - p_4$  in which the corroding specimens are described by nonlinear current-potential relationships. All the specimens were subjected to the corrosion tests for the same time of 30 min, and the voltage period was fixed at  $T = 2$  ms. The results indicate that the specimens subjected to process  $p_3$  have the best corrosion resistance and those subjected to process  $p_2$  have the worst. This is due to the fact that the energy absorbed by a given sample during the test is expressed as a multiple of the surface area of the corresponding one-period energy loop. The loops such as that shown in Fig. 3 can provide new information which could not be obtained previously when using traditional techniques such as the measurement of the open circuit potential or polarization resistance, recording the polarization curves, and/or electrochemical impedance spectroscopy [1–5]. It is evident that by applying the above tools we can predict accurately all the factors that are responsible for corrosion.

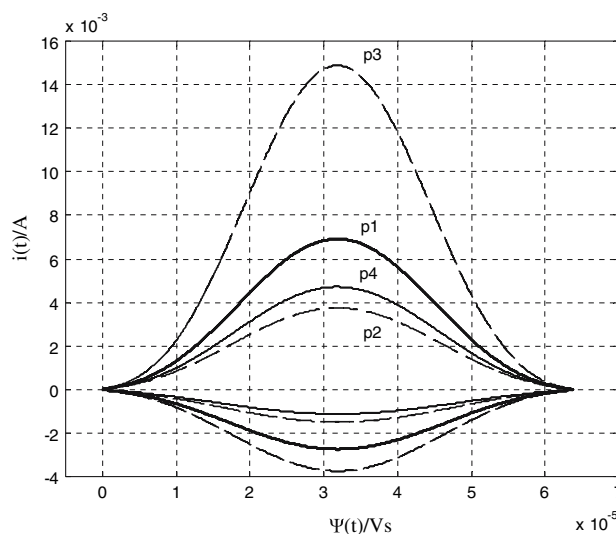


**Fig. 3** One-period energy loops for various corrosion species

**Fig. 4** Microcrystalline structure of the copper: (a) layer surface without corrosion, (b) layer surface after corrosion

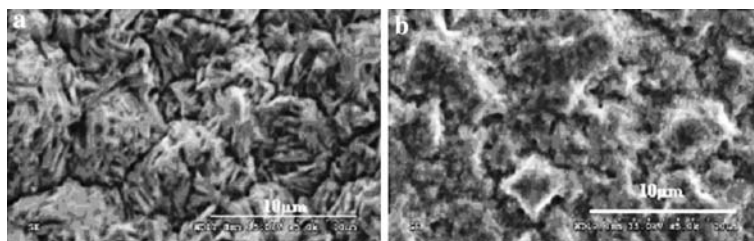
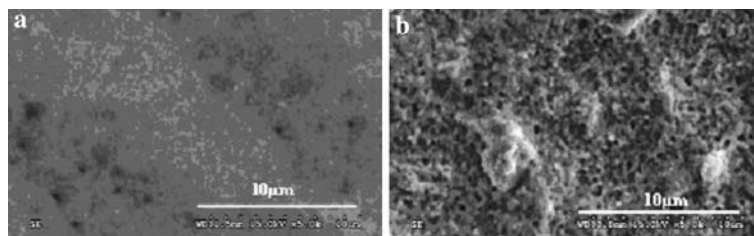


**Fig. 5** Nanocrystalline structure of the copper: (a) layer surface without corrosion, (b) layer surface after corrosion



### 3 Applications

The use of the one-period energy approach for evaluating the corrosion resistance of micro- and nano-crystalline copper thin-layers and their interactions with various corrosive environments are illustrated in Fig. 4 and Fig. 5, respectively. The SEM images shown in Figs. 4 and 5 show localized attack on a microcrystalline sample and uniform attack on a nanocrystalline structured specimen, respectively.

The layers examined in this study were deposited on polycrystalline copper substrates by the electro-crystallization method. Corrosion tests were carried out in 0.5 M NaCl using potentiodynamic polarization methods. The electrodes were thin-layer pure copper plates with an effective surface area of 1 cm<sup>2</sup>.

A large area platinum foil and a saturated calomel electrode were used as the auxiliary and reference electrodes, respectively. The working electrode was polished with 1/0, 2/0, 3/0 and 4/0 emery papers and degreased with trichloroethylene. The solutions were made using the AnalaR grade chemicals with triple distilled water.

A block diagram of the experimental setup is shown in Fig. 6. A 10 mV amplitude sine wave of a specified frequency was applied potentiostatically to the corrosion cell and the current response was analyzed by a dynamic signal analyzer. In addition, an integral of the measured

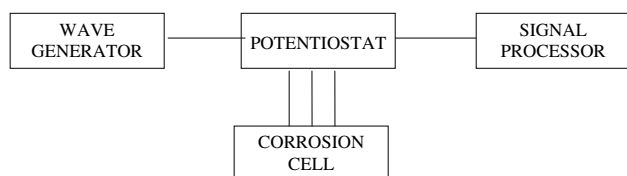


**Fig. 6** Block diagram of the experimental setup

signal was applied to the cell. For the sake of comparison, potentiostatic measurements were also performed. Generally, a uniform attack is characterized by the chemical and electrochemical reactions that proceed on the whole exposed surface. Both metals become thinner and finally undergo failure. However, in some cases, the nanostructured copper showed a lower corrosion resistance than the microcrystalline material. On the other hand the hardness and wear resistance of the nanostructured copper were better than those of the microcrystalline one.

Various morphologies of the nanocrystalline copper and microcrystalline copper are observed in the SEM images. The pitting corrosion failure of the surface of the microcrystalline copper is significant because of the smaller active intercrystalline area. Therefore, some concentrated active anode spots showed serious pitting corrosion. Stable passivation did not occur on the surface of conventional microcrystalline copper. The results of this study show that the microcrystalline surface undergoes pitting corrosion especially at the grain boundaries, impurities, triple junctions and surface defects, whereas the nano-crystalline surface is attacked by uniform corrosion.

The energy absorbed by the specimens can be easily evaluated to be:  $W_{Tmicro} = 0.844$  nJ in the nanocrystalline structures, and  $W_{Tnano} = 0.368$  nJ in the microcrystalline structures (Fig.7). Generally, the one-period energy data can be analyzed using an equivalent circuit model. The results of various interpretations of the equivalent model parameters are given in Table 1.

The model components were constructed by subtracting them successively from the measured one-period energy. The decrease of the material grain size affects the morphology and topography of the copper surface layers and increases the rate of the layer corrosion. The nanostruc-

**Table 1** Parameters of equivalent circuit elements

Copper structure	$W_T$ (nJ)	$R_c$ ( $\Omega \text{ cm}^2$ )	$C_{dl}$ ( $\mu\text{F}/\text{cm}^2$ )	$R_t$ ( $\text{k}\Omega \text{ cm}^2$ )	$C_c$ ( $\mu\text{F}/\text{cm}^2$ )	$R_c$ ( $\text{k}\Omega \text{ cm}^2$ )
$\mu\text{m}$	0.8443	10.0	8.8	1.29	58.0	7.28
nm	0.3681	13.0	7.9	3.45	77.0	7.47

tured layers exhibit lower corrosion resistance than the microstructured layers. The models of the corrosion processes provide useful information about the corrosion behavior of the crystalline copper structures irrespective of their grain size.

The electric resistance of the solution is often a significant factor that determines the impedance of the electrochemical cell. Between the counter and reference electrodes this effect can be compensated by using a modern 3-electrode potentiostat. However, the solution resistance between the reference electrode and the working electrode must be taken into account in modeling the corrosion cell.

When the electrodes are polarized by a periodic pulse voltage source, under stable conditions, the corrosion current also has a periodic form but its shape differs significantly from that of the excitation voltage. This distorted sinusoidal wave better describes the conditions that exist in practice. One can relate several properties of the corrosion system operating under sinusoidal conditions to the well-known properties of the nonsinusoidal states. By perturbing a corroding system with a distorted nonsinusoidal signal of low amplitude we do not need to perform a harmonic analysis of the current response.

The present approach can also be applied even in a nonlinear case when a given system operates in a permanent

periodic state. Taking into account the voltage input shown in Fig. 8 we can measure the one-period energy absorbed by the sample. Since both the input and output signals contain many harmonics, the one-period energy loops have different shapes than those obtained in the case of sinusoidal excitations.

The one-period energy loops obtained for the copper layers exposed to corrosion in 0.1 M NaCl are shown in Fig. 9. It can be seen that even at such a peculiar excitation as that shown in Fig. 8, the nanocrystalline copper layers exhibit worse corrosion resistance than the microcrystalline copper layers, both being exposed to the same corrosive environment. This can be verified by evaluating the energy absorbed by the individual samples during one period. This is generally attributed to the unique microstructure of the nanocrystalline materials in which the grain boundaries may occupy as much as 50% of the material volume. The corrosion rate also depends on the microstructure and such factors as the crystallographic texture, porosity, impurities and triple junctions.

A simple comparison of the absorbed energies suggest that the nanocrystalline copper layer absorbs three times as little energy as the microcrystalline copper layer. Once converted to a digital format, the output signal is then fed into a computer for analysis. Several new approaches perform most of the chip analysis by evaluating the waveforms of the output signal and computing the integral of the excitation signal. This improves the overall perfor-

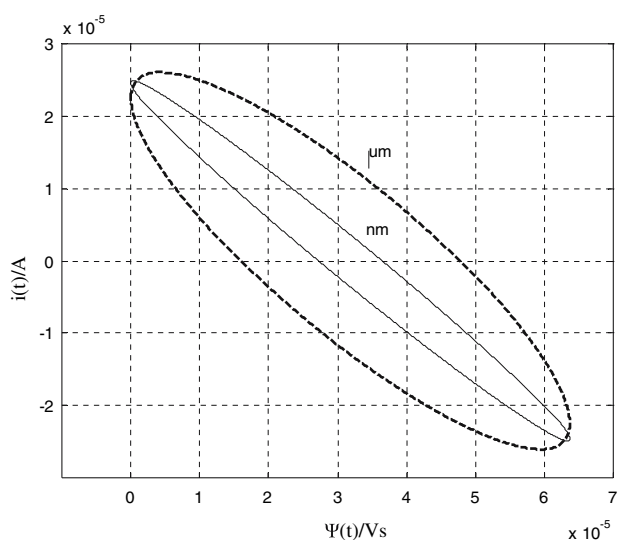


**Fig. 7** One-period energy loops for micro- and nano-crystalline layers

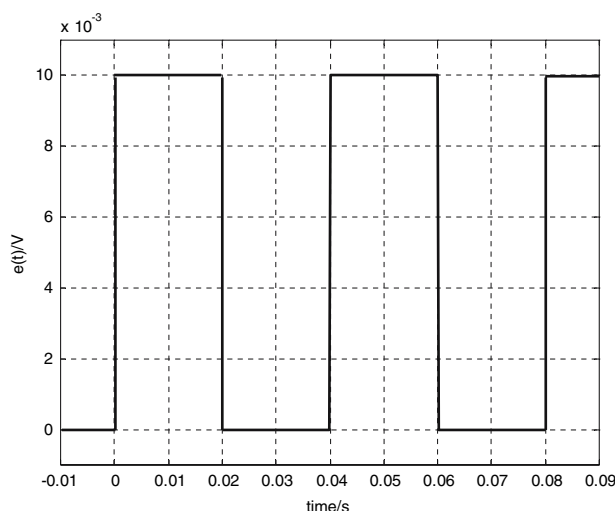


**Fig. 8** Waveform of a pulse voltage excitation

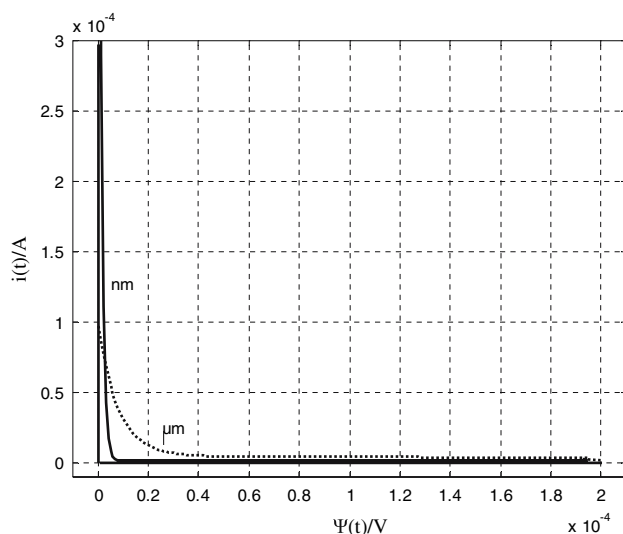


**Fig. 9** One-period energy loops under pulse voltage

mance and data collection, because the analog signal processing circuitry is functionally optimized. It is worth mentioning that, although computers can easily provide results up to four or more digits, care must be taken to ensure that the overall system remains linear. Otherwise the results will contain errors. A careful system design and its validation are critical for the desired accuracy of the experiment to be achieved.

#### 4 Conclusions

Fitting a one-period energy model to experimental data can be a straightforward task. It requires some knowledge of the corrosion cell examined, its mechanism and a basic understanding of the behavior of the cell elements. A good starting point for the development of the model is to compute the surface area of the one-period energy loop in the energy phase-plane ( $v(t)$ ,  $q(t)$ ) or equivalently ( $i(t)$ ,  $\psi(t)$ ). The corresponding integrals are denoted by  $\psi(t)$  and  $q(t)$ , respectively. This method has the advantage that the a priori knowledge of Tafel constants is not necessary and the calculation of the corrosion rate is accomplished within a very short time.

The main feature of the present approach is the total elimination of a harmonic analysis which, in turn, simplifies the appliances used for measuring the corrosion rate. The method is based on time-domain data alone and there is no need to use a second domain analysis such as, for example, the frequency domain used in the EIS method [1, 13, 17]. The use of typical mathematical tools, such as Fourier series and Fourier transforms [18] is avoided.

The usefulness of this technique has been examined for microcrystalline and nanocrystalline copper layers. We

have shown that nanocrystalline copper layers exhibit a lower corrosion resistance than microcrystalline copper ones even when they are fabricated by the same electrochemical method.

#### References

- Kelly RG, Scully JR, Shoesmith DW, Buchheit RG (2002) *Electrochemical techniques in corrosion science and engineering*. Marcel Dekker, New York
- Cha CS (2002) *Introduction to kinetics of electrode processes*, 3rd edn. Science Press, Beijing, pp 127–138
- Brett C, Brett A (1993) *Electrochemistry*. OUP, Oxford
- Welch CM, Simm AO, Compton RG (2006) *Electroanalysis* 18:965
- Tao D, Chen GL, Parekh BK (2007) *J Appl Electrochem* 37:187
- Cheng SC, Gattrell M, Guena T, Macdougall B (2006) *J Appl Electrochem* 36:1317
- Fletcher S (1994) *J Electrochem Soc* 141:18
- Darowicki K (1995) *Electrochim Acta* 40:439
- Kowalewska M, Trzaska M (2006) *J Phys Chem Mech Mater* 2(5):615
- Trzaska M, Lisowski W (2005) *Corros Prot* 48:112
- Wyszynska A, Trzaska M (2006) *J Phys Chem Mech Mater* 2(5):609
- Birbilis N, Padgett BN, Buchheit RG (2005) *Electrochim Acta* 50:3536
- Barsoukov E, Macdonald JR (eds) (2005) *Impedance spectroscopy; theory, experiment, and applications*. Wiley Interscience Publications, New York
- Macdoald JR (1990) *Electrochim Acta* 35:1483
- Bard AJ, Faulkner LR (2000) *Electrochemical methods; fundamentals and applications*. Wiley Interscience Publications, New York
- Lapicque F, Storck A, Wragg AA (1995) *Electrochemical engineering and energy. The language of science*. Springer, New York
- Dobbelaar JAL (1990) *The use of impedance measurements in corrosion research; The corrosion behavior of chromium and iron chromium alloys*, PhD thesis, Technical University, Delft
- Gabrielle C (1980) *Identification of electrochemical processes by frequency response analysis*. Solartron Instrumentation Group
- Wragg AA (1997) *J Chem Eng* 316:39
- Mansfeld F (1990) *Electrochim Acta* 35:1533
- Boukamp BA (1986) *Solid State Ionics* 20:31
- Trzaska M (2006) *Electrochemical impedance spectroscopy in corrosion studies of copper surface layers Proc VII Intern Workshop 'Computational Problems of Electrical Engineering'*, Odessa, Ukraine
- Shinohara K, Aogaki R (1999) *Electrochem* 67:126
- Trzaska Z, Marszalek W (2006) *Periodic solutions of DAEs with applications to dissipative electric circuits, Proc IASTED Conf Modelling, Identification and Control (MIC06), Lanzarote, Spain*
- Trzaska Z (2004) *Arch Elec Eng* 53:191
- Trzaska Z (2005) *Arch Elec Eng* 54: 265
- Trzaska Z, Marszalek W (1993) *IEE Proc PtD, Control Theory Appl* 140:305
- Trzaska Z, Marszalek W (2006) *Arch Elec Eng* 55:165
- Farkas M (1994) *Periodic motion*. Springer-Verlag, New York
- Chian HD, Chu CC, Cauley G (1995) *Proc IEEE* 831: 497
- Chun-Lei T, Wu X-P (2004) *Proc Amer Math Soc* 132:1295
- Mhaskar HN, Prestin J (2000) *Adv Comput Math* 12:95
- Bartle RG, Sherbert D (1997) *Introduction to Real Analysis*, 2nd edn. Wiley, New York